WORK CARRIED OUT AT THE ESRF TO CHARACTERISE AND CORRECT THE COUPLING

R. Nagaoka, ESRF, Grenoble, France

Abstract

An attempt has been made at the ESRF to model the linear coupling with the measured coupled-orbit response. Rather than pursuing an individual magnet skew error, the aim was to obtain an effective skew error distribution that describes the measured coupling characteristics. Such a solution was actually found, assured by the simulation taking the ESRF steerer-BPM configuration, as well as by the excellent BPM accuracy. Finding it effective to correct the coupling by minimising the model coupling, the most effective skew correctors were searched for and additionally installed. It has been found that a smaller coupling does not always result in a smaller coupled-orbit response. The vertical emittance of less than 10 pm·rad is finally achieved with the help of X-ray pinholes, capable of measuring the vertical emittance of several picometres, in the regime where the magnitude of the coupled-orbit response is already too small to be utilised. Studies are made of the effect of vertical beam motions that could saturate the coupling correction. Attempts to remove peaks of the skew error distribution with magnet displacement, to clarify the sextupole contribution to skew errors, as well as to measure the coupling with thousand-turn BPMs are also presented.

1 INTRODUCTION

One of the major performances of third generation light sources such as the ESRF consists in realising smaller transverse beam sizes, namely emittances, by orders of magnitude as compared to the previous generation. This comes from the fact that the brilliance of the photon beam is inversely proportional to the electron beam emittances. Here, the term *coupling* refers strictly to the ratio of the vertical emittance to the horizontal, as it is the net vertical beam size that is the relevant parameter for the beamlines. As we shall see below, however, the coupling for the ESRF machine is nearly equivalent to the *betatron coupling*, as the contribution of the vertical dispersion to the vertical emittance is found to be negligible. The coupling at the ESRF has been corrected to less than 1% for the daily operation, reducing the uncorrected coupling of approximately 10% with 16 skew correctors. Focusing upon the fact that the coupled-orbit response, otherwise called the orbit cross-talk (OCT), results from the linear coupling, the correction starts from minimising the OCT to a certain degree, which provides a good base for the subsequent correction of sum and difference resonances.

With the aim of going further down to the level of 0.1% coupling, the above fact motivated us to study the relation between the OCT and the coupling in more detail, along with the general minimisation of OCTs [1]. Meanwhile, an accurate calibration of quadrupoles was carried out using the diagonal part of the response matrix, which triggered our second motivation to extract the effective skew errors from the OCT, as a natural extension of the work on the diagonal matrix. In whichever case, the attempt to make use of the orbit response matrix to perform the coupling correction is based upon the fact that the ESRF BPMs have a micron reading accuracy, as well as upon the quantity of information contained in the matrix.

2 MODELLING OF A LINEARLY COUPLED MACHINE

2.1 Formulation

Writing down the transversely coupled equations of the orbit response due to steerer excitations, one finds that skew quadrupole strengths appear linearly in the dipolar terms of the equation in the plane orthogonal to the steerer excitation. Namely, a horizontal shift of the orbit with *j*th horizontal steerer by $\Delta\theta_{Hj}$, for example, associates a vertical orbit shift $\Delta \mathbf{z}_{CO}$, which follows the relation represented in the matrix notation as

$$\frac{\Delta z_{CO}}{\Delta\theta_{Hj}} = \mathbf{R}_{ik}^{(V)} \cdot \mathbf{R}_{kj}^{(H)} \cdot \mathbf{a}\,, \qquad (1)$$

where **a** represents an array of skew components, the positions of which are defined by the model. $R^{(H)}{}_{kj}$ and $R^{(V)}{}_{ik}$ are respectively, the horizontal response matrix from steerer *j* to skew quadrupole *k*, and the vertical response matrix from skew quadrupole *k* to BPM *i*. One can assume that these elements are known accurately from the diagonal matrix analysis. The skew strengths can thus be solved simply via the matrix inversion (e.g. SVD method). This feature may be contrasted with the diagonal case, in which the unknown dipolar errors are already subtracted off in the *original* orbit. Also regarding the quadrupole errors ΔQ_k's, the corresponding relation is not linear, as can be seen in the horizontal equation below,

$$\frac{\Delta x_i}{\Delta \theta_{Hj}} = A_{ij}^{(H)}(\boldsymbol{Q_0}) + \sum_k \frac{\partial A_{ij}^{(H)}}{\partial Q_k} \cdot \Delta Q_k + \ldots \quad (2)$$

Here, $A^{(H)}_{ij}(\boldsymbol{Q_0})$ denotes the model horizontal response matrix with known quadrupole strengths $\boldsymbol{Q_0}$. As a result, the equations are normally solved iteratively [2]. To study the effectiveness of methods using Eq. 1, simulations were performed for the specific ESRF steerer-BPM-skew corrector configuration.

2.2 Simulation

Minimisation of OCT and its relation with the coupling are firstly discussed: By taking $\boldsymbol{a}$ as skew correctors in Eq. 1, one can compute their strengths that compensate the OCT generated by jth steerer. As may be anticipated, however, these solutions are found to be fully j-dependent, with some even increasing the coupling. Instead, through a general least square method, a set of solutions $\boldsymbol{a}$ can be readily found that reduces the overall OCT. A noteworthy finding here is that, none the less, the reduced OCTs do not necessarily produce smaller couplings. The relation apparently depends sensitively on the steerer-BPM-skew corrector configuration chosen. In the ESRF case, the best solutions for the coupling are found even to *increase* the OCT. It was shown in Ref. 3, that in the limit of a sufficiently large number of skew correctors distributed, the minimisation of OCT does become equivalent to the coupling correction. Though OCTs and the betatron motions satisfy the same coupled equations, the fact that the former are special periodic solutions is suspected to be the underlying reason for this non-trivial relation.

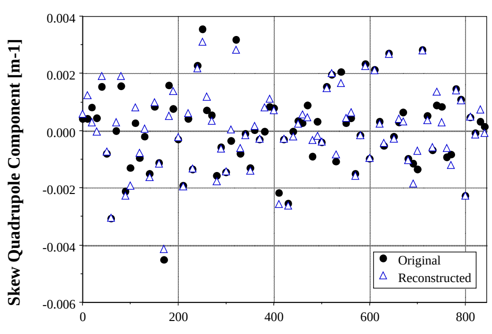

Figure 1: Locally integrated skew strengths (every 10 meters) between the original and reconstructed machines.

The above findings led us to employ Eq. 1 to extract the skew error distribution rather than minimising OCTs, since there is only a limited number of skew correctors in reality. Solving Eq. 1 for the specific ESRF configuration, we find that there is not a good enough resolution to identify a single magnet skew error, namely a tilt error of a quadrupole or a vertical displacement (or closed-orbit) error of a sextupole. However, locally integrated strengths can be well reproduced (Fig. 1), with which the coupling of the original machine can be described locally and globally in a satisfactory manner. In contrast to the earlier work made on the same principle [2], we may stress here the importance of building an *effective skew distribution* to characterise the linear coupling, as well as to perform the correction on the basis of the obtained model. It also conforms with the fact that the skew errors arising from sextupoles are comparable in magnitude to the quadrupole tilts for the ESRF machine.

The simulation code makes normal mode decomposition on a 4×4 one-turn transfer matrix to derive the normal mode coupling, the betatron coupling coefficient κ and its corresponding emittance ratio g due to the nearest difference resonance. Among position-dependent quantities computed along the machine are the geometric coupling, what we call the beam size deduced coupling, as well as the tilt angle of the beam ellipse. The beam size deduced coupling best corresponds to the emittance ratio computed from the actual beam size measurement. The simulated routine starts from the response matrix acquisition on a given *original* machine with errors, and extracts the skew error distribution to get the *reconstructed* machine. The coupling correction of the *original* machine is then made by acting on the *reconstructed* machine, using any of its coupling parameters as they are *known*.

2.3 Application to the Real Machine

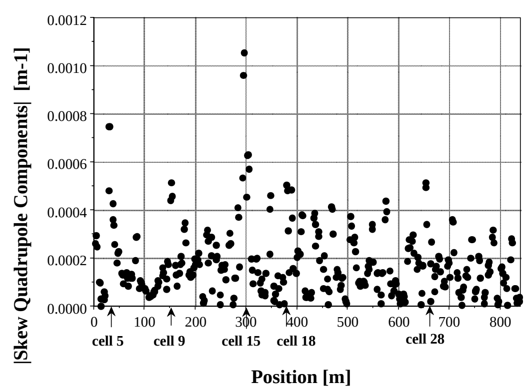

Figure 2: Skew distribution of the uncorrected coupling.

Unlike the simulation, the effect of averaging turned out to be particularly important in removing the imperfections contained in the measured matrices. Equation 1 is solved with the SVD method taking a set of data corresponding to a pair of steerers belonging to the same family optics wise. The obtained skew distribution is then averaged over the entire pairs and families. Besides reading errors, averaging helps remove possible tilt errors of steerers and BPMs, which create false components in the skew distribution. Search for the most appropriate number of eigenvectors is found equally important, which however appears to be a constant of the correction system. Most computations were made by placing the skew flags at quadrupoles (10 flags per cell). Although valid solutions can be obtained with fewer flags, it tends to increase the magnitude of individual skew strengths. The measured OCTs are reproduced typically to few microns rms.

The resultant skew distribution of the machine without coupling correction exhibits several localised peaks (Fig. 2). Assuming that the skew errors come from quadrupole rotation errors, the rms tilt angle is computed to be θ_{rms} = 0.35 mrad, which indicates that the peaks are too large to be girder rotation errors. Attempts to remove these peaks are described in Sec. 5.

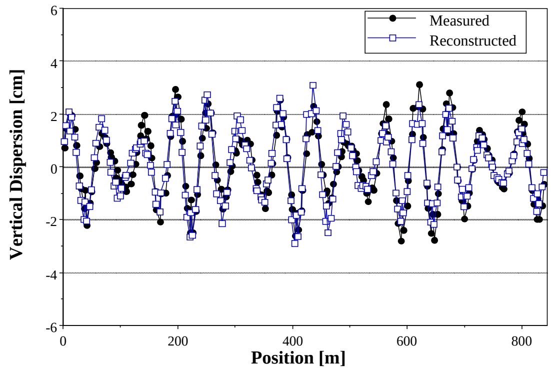

Figure 3: Comparison of vertical dispersion of the uncorrected coupling, between measured and calculated.

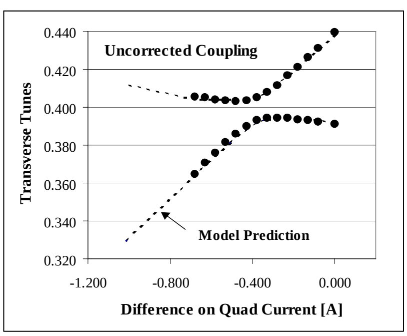

Figure 4: Predicted tune separation of the uncorrected coupling, in comparison with the measured one.

The skew distribution reproduces well the measured vertical dispersion (Fig. 3), as well as the tune separation around the coupling resonance (Fig. 4), i.e. the two principal properties of the coupling. The normal mode coupling comes out as 4.6%, while the geometric coupling is about 7.5% on the average, which is much larger than 4.6% coming from the nearest difference resonance (= g). The good reproduction of the vertical dispersion (Fig. 3) signifies that the emittance coupling of the ESRF machine is mostly the betatron coupling, as the model takes no account of vertical dipolar kicks that additionally generate the vertical dispersion.

3 COUPLING CORRECTION

As in the simulation, the correction of coupling was attempted with the effective skew error distribution of the ESRF machine using the existing 16 skew correctors. The resulting corrector strengths agree well with those actually obtained from the standard correction.

To reduce further the coupling, a search was made for the most effective corrector positions with respect to the specific non-uniform skew errors. Placing 96 skew correctors around the model machine at allowed locations, minimisation of the normal mode coupling was made with the best corrector method, taking account of the correlation among the selected correctors. A large reduction to 0.05% was obtained on the normal mode coupling with 16 best correctors, as compared to 0.3% with the existing correctors (Fig. 5). Interestingly, the OCT is simultaneously reduced in the optimised correction. Figure 6 summarises the relation between the coupling and the OCT, for the three representative coupling conditions: 1) Uncorrected. Best corrected with 2) the existing correctors, and with 3) the 16 most effective correctors.

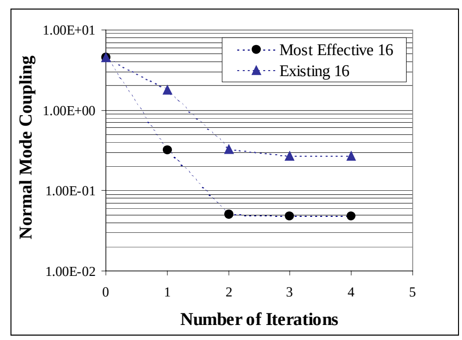

Figure 5: Correction efficiency of the most effective correctors, in comparison with the existing ones.

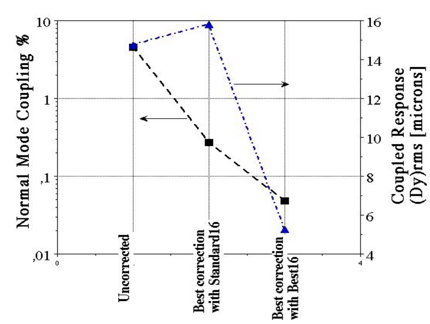

Figure 6: Relation between the coupling and the OCT for three different correction states described in the text.

The study led 16 additional skew correctors to be installed in the ring. Actual application of the model solution expectedly realised a lower coupling than the standard correction. The remaining discrepancy with the predicted value is supposedly attributed mostly to inaccuracies of the model. A difficulty was encountered here, however, that as a consequence of the reduced coupling, the OCT is now too small to iterate the procedure. As the only remaining, yet promising alternative, use of the X-ray pinhole measurement was considered. The installed pinholes, which utilise the bending magnet radiation, are capable of measuring the vertical emittance to less than 5 pm·rad [4]. The simulation finds that, starting from the model solution with proper weighting on the vertical dispersion, minimisation of the vertical beam size measured at two locations in the ring (ID8 and D9) leads to the minimal coupling. It was in this way that the record value of 9 pm·rad, i.e. a coupling of less than 0.25%, was actually achieved as measured on both pinholes (Fig. 8). In accordance with the prediction, the measured OCT was significantly reduced (the rms is 5 µm against 4 µm of predicted). Together with the vertical dispersion which is reduced to 0.3 cm rms (instead of 0.15 cm predicted), the reached setting is expected to be in the vicinity of the best point.

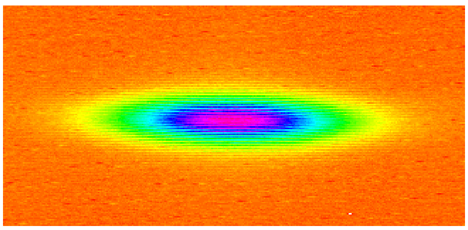

Figure 7: The beam image from the X-ray pinhole at the smallest coupling (< 0.25%). Note that the beta values at the source points are approximately 2.7 m horizontally and 35 m vertically.

4 SOME ASPECTS OF THE ELECTRON BEAM AT THE SMALLEST COUPLING

Through the empirical corrections, it was experienced that the correction saturates before reaching the vertical emittance of 10 pm·rad level in apparently non-reproducible manner. After investigations, the cause was found to be vertical beam motions, which can be classified into two categories: 1) Fast vertical oscillations of the orbit. 2) Vertical beam instabilities. The former significantly disturbs the beam size measurement as the coupling is reduced. The capability of varying the integration time between 20 to 1 ms in the pinhole measurement allowed the effect to be quantified. The global orbit feedback helps to keep the measured vertical emittance to a smaller value.

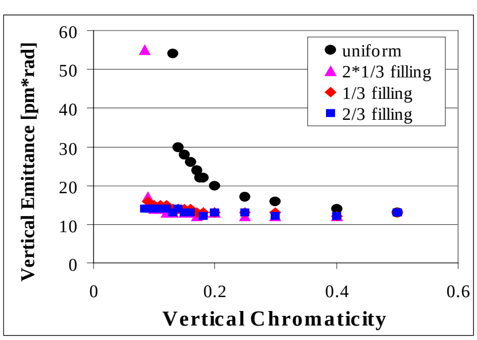

Figure 8: Influence of vertical instabilities on the vertical emittance, for different filling patterns.

On the other hand, it required more effort to characterise the latter effect. The correlation of the vertical instability to the vertical emittance shown in Fig. 8 explains the long existed puzzle for the aforementioned non-reproducibility. The instabilities are considered to be resistive-wall and ion trapping, whose influence varies according to the filling pattern [5]. It explains that a better correction can be performed in a partial filling at high current, where there is more stability against coherent motions.

The reduction of Touschek limited lifetime for smaller couplings is found to be roughly up to 10 hours, under the standard multibunch operation at 200 mA, in agreement with the expectation. Although the sensitivity to insertion device gap variations enhances for smaller couplings, an update of the empirical correction well compensates their effects. In the low coupling operation tentatively introduced for beamline users, the correction procedure was automated and kept running so as to start the correction as soon as the measured vertical beam sizes exceed a certain threshold. The vertical emittance was in most times kept between 9 to 11 pm·rad with 200 mA beam in 2×1/3 filling. Actual ID gap variations did not bring vertical emittances beyond ~15 pm·rad level.

5 FURTHER DEVELOPMENT

5.1 Removal of Largest Skew Errors

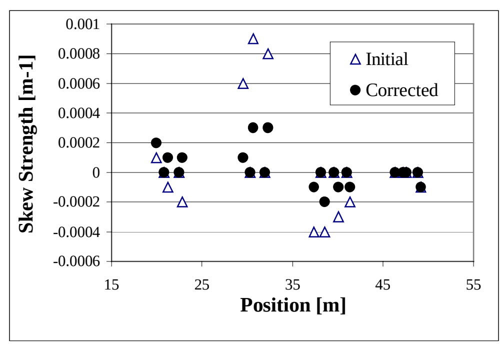

Figure 9: Measured reduction of the peak amplitude of the skew errors in Cell 5.

With non-uniformity revealed in the effective skew error distribution, an attempt was made to eliminate the two largest peaks in the distribution (cell 5 and 15 in Fig. 2) by moving the magnets. As there is no resolution to identify a wrong magnet, among the two equivalent actions of rotating a quadrupole and vertically displacing a sextupole, the latter was chosen for the reason of feasibility. Displacing three sextupoles by nearly 0.5 mm in the proper directions, both peaks were successfully removed to a good extent (Fig. 9), which reduced the geometric coupling of the uncorrected machine from 7.5 to 4%, enabling the standard correction to reach a lower vertical emittance (20 pm·rad).

5.2 Sextupole Contribution to Skew Errors

Efforts have been made to distinguish the contribution of sextupoles to the skew errors from the quadrupoles. By exploring sextupole settings with a sufficiently large difference on a single family, keeping feasibility of beam accumulation, the skew error analysis is repeated singling out the chosen sextupole family. Namely, Eq. 1 is solved with the difference of the two measured matrices with skew flags only placed at the selected sextupoles. Analysis was made so far over the four harmonic sextupole families. The peak seen in the distribution shown (Fig. 10) consistently represents the displacement made on this family member to compensate the largest skew error (Subsec. 5.1). Measured response matrices can be applied in the same way to the analysis of quadrupole errors (i.e. optical asymmetry).

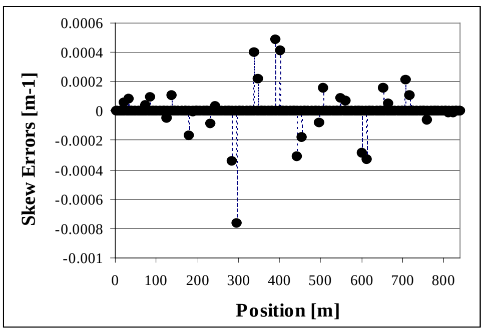

Figure 10: Skew errors found for a sextupole family.

5.3 *Coupling Measurement with Thousand-Turn BPMs*

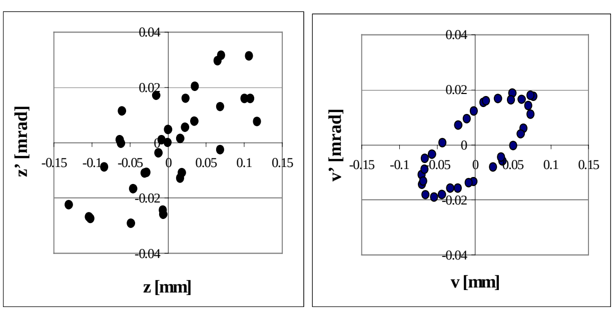

Figures 11: Vertical phase space (left) and normal mode phase space (right), obtained from the thousand-turn BPM measurement.

A system called *Mille-Tour BPMs* [6] was recently implemented at the ESRF that reconstructs turn-by-turn readings from those of the individual pickup electrodes. Although application is limited to reproducible motions, averaging together with the excellent reading accuracy of the ESRF BPMs achieves a highly accurate reading on the turn-by-turn basis. As an interesting application, the measurement of coupling has been attempted. The steps developed are as follows: For each straight section that has no focusing element in between two BPMs, 1) Construct the phase space (x, x', z, z'). 2) Fit the phase space data to extract a 4×4 one turn matrix. 3) Perform normal mode decomposition to get the normal mode coupling, followed by deduction of position dependent couplings. Step 2 is found to be the most non-trivial, especially as the number of available turns is severely limited due to the strong decoherence of the beam. The first result obtained nevertheless seems promising (Figs. 11), giving a normal mode coupling of 1.1%, in a reasonable range with respect to the measured coupling of 2.2%. The advantage of this approach is clearly the quantity of available data around the machine, besides its independent and well-defined measurement. Depending upon the applicability for smaller couplings, a new correction scheme could be envisaged.

6 CONCLUSION

The scheme developed to use the orbit cross-talk (OCT) to obtain the effective skew error distribution turned out to give a sufficiently accurate description of the linear coupling of the ESRF machine. The most effective correction with the installation of new correctors, followed by the use the X-ray pinholes to reach the final minimum, has successfully reduced the coupling of the ESRF machine by nearly a factor of three to less than 0.25%. Additional efforts have been made to understand the effect of vertical beam motions that limit the ultimate coupling correction, as well as the content of the obtained skew errors. Elimination of the largest peaks in the skew errors was successfully made by displacing the sextupoles. A new attempt is underway to describe and correct the coupling using the thousand-turn BPMs.

ACKNOWLEDGEMENT

The author is especially grateful to his colleague Laurent Farvacque, who has collaborated with him at all stages of the work. He thanks Jean-Luc Revol for his collaboration on the study of instability effects on the coupling. Thanks are also to all those who supported this work from different groups at the ESRF.

REFERENCES

[1] R. Nagaoka, "Modelling of a Linearly Coupled Machine Using the Coupled-Response Matrix", EPAC98, Stockholm, June 1998.
[2] J. Safranek, "Experimental Determination of Storage Ring Optics Using Orbit Response Measurements", Nucl. Instr. And Meth., A388 (1997) 27.
[3] P. Nghiem and M.A. Tordeux, "Coupling Correction for the ESRF", SOLEIL report, March 1999.
[4] P. Elleaume, C. Fortgang, C. Penel and E. Tarazona, "Measuring Beam Sizes and Ultra-Small Electron Emittances Using an X-ray Pinhole Camera", J. Synchrotron Rad., **2** (1995) 209.
[5] R. Nagaoka, J.L. Revol, J. Jacob, "Observation, Analysis and Cure of Transverse Multibunch Instabilities at the ESRF", this conference.
[6] K. Scheidt, private communication.